J. Am. Chem. Soc. 1990, 112, 5731-5735 5731

Theoretical Study of Reactivity of Methane, Methyl Fluoride, and Methyl Chloride: Interaction with Their Radical Cations and Proton Donors

B. Andes Hess, Jr.,*,† and Rudolf Zahradník*,‡

Contribution from the Department of Chemistry, Vanderbilt University, Nashville, Tennessee 37235, and the J. Heyrovský Institute, Dolejškova 3, Czechoslovak Academy of Sciences, 18 223 Prague 8, Czechoslovakia. *Received December 14, 1989*

Abstract: This work deals with interactions between CH_4 and $CH_4^{\bullet+}$, CH_3F and $CH_3F^{\bullet+}$, and CH_3Cl and $CH_3Cl^{\bullet+}$. The calculated ΔH_0 values (MP4/6-31G**//MP2/6-31G**, ZPE included) for processes leading to CH_5^+ and $CH_3^{\bullet}$, and to CFH_4 and $CH_2F^{\bullet}$ amount to −1.8 and −21.0 kcal/mol, respectively. That ΔH_0 leading to $CClH_4^+$ and $CH_2Cl^{\bullet}$ (MP4/6-31G** //SCF/6-31G**, ZPE included) is −2.3 kcal/mol. The calculated reaction heat for the first interaction is significantly closer to experimental values (−4.16 and −6 kcal/mol, respectively) than our previous theoretical estimates. The structures of the radical cations ($CH_4^{\bullet+}$, $CH_3F^{\bullet+}$, $CH_3Cl^{\bullet+}$) possess features of van der Waals associates. Methyl fluoride forms a weak hydrogen-bonded complex with HF the structure of which is, in contrast to expectation based on simple electrostatic consideration, nonlinear. The structure of the $CH_3Cl{\cdot}HCl$ complex is analogous, but the ΔH_0 value is very low (−0.1 kcal/mol).

I. Introduction

Ion–molecule reactions have attracted considerable attention from experimentalists over the last three decades,[1] but on the other hand only a small number of theoretical studies are available. This is rather astonishing since quantum chemical methods can significantly facilitate their understanding, e.g., energy considerations and structural assignments for intermediates as well as for products of such reactions. Such studies would be useful for the prediction and interpretation of reactions in molecular beams as well as photochemical studies of ion–molecule processes taking place at low temperature in inert matrices.

The main purpose of this study is to obtain energy profiles for reactions between methyl fluoride and chloride and their radical cations

$$CH_3X + CH_3X^{\bullet+} \rightleftarrows C_2H_6X_2^{\bullet+} \rightleftarrows CH_4X^+ + CH_2X^{\bullet} \quad (1)$$

where X = F and Cl. This work is related to our papers on simple hydrides[2] and on extensive sets of simple ion–molecule reactions.[3] Our effort has been intensified due to a recent report[4] on the experimental investigation of the reaction shown in eq 1 (X = F).

The reaction between CH_3Cl and its radical cation was studied by Suzuki and Koyano using the threshold electron-secondary ion coincidence (TESICO) technique.[5,6] The peaks found in the time-of-flight coincidence spectra of the product ion, CH_4Cl^+, were interpreted in terms of participation of proton and hydrogen atom transfer mechanisms in the formation of CH_4Cl^+. It was shown that the cross sections for these two processes are approximately of the same size.

Although the parent reaction[1,7] (eq 2) has been studied previously,[8,9] we felt it desirable

$$CH_4 + CH_4^{\bullet+} \rightleftarrows C_2H_8^{\bullet+} \rightleftarrows CH_5^+ + CH_3^{\bullet} \quad (2)$$

to reinvestigate this interaction at the same level as that of the related reactions studied here. Possible configurations of the $C_2H_8^{\bullet+}$ intermediate were discussesd long ago,[10] and it was shown[8] that on the potential energy surface of the intermediate $C_2H_8^{\bullet+}$, there exist numerous stationary points. Although it is possible to obtain for cation–molecule reactions rather reliable quantum chemical information at the SCF level (even with a small basis set), it is desirable to verify the original energetic and structural predictions[8] at a substantially higher level. It is even more topical because of a very recent study[11] in which a set of radical cation dimers, $(M)_2^{\bullet+}$, was formed by coupled "switching-type" reactions. The special value of this technique is that it allows one to prepare $(M)_2^{\bullet+}$ species even in the case where a direct interaction between M and $M^{\bullet+}$ is so exothermic that it leads directly to fragmentation products.[11]

In the gas phase the rate constants of proton-transfer reactions reach a value of 25 × 10^{-10} cm^3/molecule·s, i.e., their rate approaches the collision rate. This applies to all three reactions studied here that involve $CH_4^{\bullet+}$ (ref 12), $CH_3F^{\bullet+}$ (refs 13–15), and $CH_3Cl^{\bullet+}$ (refs 13 and 15). These and related processes are discussed together with other processes involving the same structural type, i.e., $CH_3X^{\bullet+}$ cations.[1]

Finally in connection with the analysis of high-resolution infrared spectra a question was asked[16] concerning the geometry of the hydrogen-bonded complex between methyl fluoride and hydrogen fluoride. This complex and the analogous chlorine-containing complex are also studied.

II. Calculations

The geometry optimization and vibrational frequency calculations were carried out at the SCF/6-31G** and MP2/6-31G** levels for hydrocarbons and fluorine-containing species (I–XI) with the exception of the intermediate $(CH_3F)_2^{\bullet+}$ (XII) whose frequencies were obtained at the SCF level; only the former level has been used for chlorine-containing systems (XIII–XVIII). Moreover, for all optimized structures single-point MP2, MP3, and MP4 and CCD calculations were performed. Geometries, energies, and zero-point energies (ZPE) are presented in Tables I and II for all the species included in Figure 1 as well as for additional stationary points on the $CH_3F{\cdot}HF$ potential energy surface (first-order saddle point, XIa, and second-order saddle point, XIb). Characteristics for methane and methyl fluoride and their deriv-

---

† Vanderbilt University.

‡ Czechoslovak Academy of Sciences.

(1) Lias, S. G.; Ausloos, P. *Ion–Molecule Reactions*; American Chemical Society: Washington, DC, 1975.

(2) Zahradník, R.; Havlas, Z.; Hobza, P.; Hess, B. A., Jr. *Collect. Czech. Chem. Commun.* **1990**, *55*, 0000.

(3) Herman, Z.; Zahradník, R. *Collect. Czech. Chem. Commun.* **1989**, *54*, 2910.

(4) Suzuki, S.; Koyano, I. *Annu. Rev., Inst. Mol. Sci., Okazaki* **1988**, 78.

(5) Suzuki, S.; Koyano, I. *Int. J. Mass Spectrom. Ion Proc.* **1987**, *80*, 187.

(6) Suzuki, S.; Koyano, I. *Radiochim. Acta* **1988**, *43*, 115.

(7) Herman, Z.; Friedrich, B.; Henchman, M. J. *J. Chem. Phys.*, In press.

(8) Havlas, Z.; Bauwe, E.; Zahradník, R. *Chem. Phys. Lett.* **1985**, *121*, 330.

(9) Kamiya, K.; Morokuma, K. *Chem. Phys. Lett.* **1986**, *123*, 331.

(10) Field, D.; Gray, N. A. B.; Knewstubb, P. F. *J. Chem. Soc., Faraday Trans. II* **1972**, *68*, 852.

(11) Smith, D.; Adams, N. G. *Chem. Phys. Lett.* **1989**, *161*, 30.

(12) Buttrill, S. E., Jr. *J. Chem. Phys.* **1969**, *50*, 4125.

(13) Beauchamp, J. L.; Holtz, D.; Woodgate, S. D.; Patt, S. L. *J. Am. Chem. Soc.* **1972**, *94*, 2798.

(14) Marshall, A. G.; Buttrill, S. E., Jr. *J. Chem. Phys.* **1970**, *52*, 2752.

(15) Herod, A. A.; Harrison, A. G.; McAskill, N. A. *Can. J. Chem.* **1971**, *49*, 2217.

(16) Papousek, D.; personal communication, 1989.

0002-7863/90/1512-5731$02.50/0

Table I. Geometries and Energies

molecule[b]	parameter	geometry and energy[a] MP2/6-31G**//MP2/6-31G**[c]
CH_4 (I)	R_{C-H}	1.0843
(T_d)	energy	−40.36986
	ZPE	0.04661
$CH_4^{\bullet+}$ (II)	R_{C-H}	1.0784
(C_{2v})	$R_{C-H'}$	1.1737
	$\angle_{HCH}$	125.0
	$\angle_{H'CH'}$	54.6
	energy	−39.90778
	ZPE	0.04005
CH_5^+ (III)	R_{C-H1}	1.1772
(C_s)	R_{C-H3}	1.1023
	R_{C-H4}	1.0834
	$\angle_{H1CH2}$	47.9
	$\angle_{H2CH3}$	75.8
	β^d	129.0
	$\angle_{H4CH5}$	119.5
	energy	−40.58028
	ZPE	0.05351
$CH_3^{\bullet}$ (IV)	R_{C-H}	1.0734
(D_{3h})	energy	−39.69753
	ZPE	0.03076
$CH_3-H\cdots H-$	$R_{C-H'}$	1.2413
$CH_3^{\bullet+}$, (V)	R_{H-H}	0.9718
(D_{3d})	R_{C-H}	1.0831
	$\angle_{HCH'}$	100.7
	energy	−80.30049
	ZPE	0.08917[d]
CH_3F (VI)	R_{C-F}	1.3877
(C_{3v})	R_{C-H}	1.0872
	$\angle_{HCF}$	109.3
	energy	−139.36744
	ZPE	0.04074
$CH_3F^{\bullet+}$ (VII)	R_{C-F}	1.2927
(C_s)	R_{C-H}	1.0811
	$R_{C-H'}$	1.1565
	$\angle_{FCH}$	116.9
	$\angle_{H'CH'}$	76.4
	α^f	115.3
	energy	−138.91273
	ZPE	0.03396
CH_3FH^+ (VIII)	R_{C-F}	1.6006
(C_s)	R_{F-H}	0.9517
	R_{C-H}	1.0789
	$R_{C-H'}$	1.0796
	$\angle_{CFH}$	115.3
	$\angle_{FCH}$	98.5
	$\angle_{FCH'}$	102.5
	$\angle_{HCFH}$	180
	$\angle_{H'CFH}$	60.9
	energy	−139.612260
	ZPE	0.05057
$CH_2F^{\bullet}$ (IX)	R_{CF}	1.3481
(C_s)	R_{CH}	1.0772
	$\angle_{FCH}$	114.3
	$\angle_{HCH}$	121.9
	energy	−138.70254
	ZPE	0.02597
H−F (X)	R_{H-F}	0.9210
($C_{\infty v}$)	energy	−100.19670
	ZPE	0.00955
$CH_3F\cdots HF$	R_{C-F1}	1.4095
(XI)	R_{F1-H1}	1.7526
(C_s)	R_{H1-F2}	0.9291
	R_{C-H2}	1.0831
	R_{C-H3}	1.0846
	$\angle_{CF1H1}$	102.0
	$\angle_{F1H1F2}$	154.1
	$\angle_{F1CH2}$	107.8
	$\angle_{F1CH3}$	108.2
	$\angle_{H3CF1H1}$	120.1
	energy	−239.57828
	ZPE	0.05375
$CH_3F\cdots HF$	R_{C-H1}	1.0802
(XIa)[d]	R_{C-H2}	1.0801
(C_s)	R_{C-F1}	1.3818
	R_{F1-H4}	1.8285
	R_{F2-H4}	0.9057
	$\angle_{H1CF1}$	108.1
	$\angle_{H2CF1}$	108.5
	$\angle_{CF1H4}$	105.8
	$\angle_{F1H4F2}$	152.6
	$\angle_{H4F1CH2}$	59.9
	energy	−239.06174
$CH_3F\cdots HF$	R_{C-H1}	1.081
(XIb)[d]	R_{C-F1}	1.377
(C_{3v})	R_{F1-H4}	1.890
	F_{F2-H4}	0.904
	$\angle_{H1CF1}$	108.5
	energy	−239.05954
$FCH_2-H\cdots$	$R_{H'-H'}$	0.981
$HCH_2F^{\bullet+}$	$R_{C-H'}$	1.265
(XII)	R_{C-H}	1.087
(C_{2h})[c]	R_{C-F}	1.316
	$\angle_{H'CH}$	99.8
	$\angle_{H'CF}$	106.3
	$\angle_{H'H'C}$	163.5
	$\angle_{HCH'F}$	119.0
	$\angle_{H'H'CF}$	0.0
	energy	−278.30277
	ZPE	0.07855[d]

[a] Energies are in au, bond distances in Å, angles in deg. [b] See figure for definition of atoms. [c] MP2 energies are with full core. [d] SCF/6-31G**//SCF/6-31G**. [e] Angle made by C–H3 and the bisector of the H4–C–H5 plane. [f] Angle made by F–C and the bisector of the H–C–H plane.

atives are given in Table I and those for methyl chloride and its derivatives in Table II. Basis set superposition errors (BSSE) were calculated by using the function counterpoise method for complexes V, XI, XII, and XVIII. All the calculations were done with the GAUSSIAN 86[17] and CADPAC[18] programs.

III. Results and Discussion

Ionization Potentials. In spite of the fact that ionization potentials for CH_4, CH_3F, and CH_3Cl have been repeatedly studied theoretically, we have also computed these since geometries of these systems were optimized at the MP2 level; both vertical and adiabatic potentials were calculated. From Table III it is seen that the agreement between calculated and observed values is quite good, significantly better than at the commonly used simpler theoretical levels.

Proton Affinities. In Table IV three of the calculated energies of protonation are compared with experimental protonation enthalpies at 298 K, and the three additional values represent predictions. (Table IV). The agreement between calculated and observed values is reasonably good. The inclusion of the enthalpy change when passing from 0 K to 298 will not change significantly the result. The origin of the discrepancy might also lie with experiment; the two significantly different published values of proton affinities for CH_3F support this view.

From a study by Baumgärtel et al.[23] on the photodissociation of CH_3F clusters, heats of formation of a set of fluorine-containing species are available. These values were corrected to 0 K and permit a direct comparison with our calculated values. The calculated protonation energy of CH_3F, −155.2 kcal/mol, differs by about 4% from a value obtained from the $\Delta H_f(0\ K) = -149.2$ kcal/mol. When using from the same set of $\Delta H_f(0\ K)$ values data for the HF dissociation, $HF \rightleftarrows H^+ + F^-$, a value of 370.0 kcal/mol is obtained, which is in poor agreement with the MP4/6-31G**//MP2/6-31G** value, 415.3 kcal/mol (ZPE included).

The CH_4–$CH_4^{\bullet+}$, CH_3F–$CH_3F^{\bullet+}$, and CH_3Cl–$CH_3Cl^{\bullet+}$ Interactions. In our previous study[8] eleven stationary points were located on the 3-21G potential energy surface of the CH_4–$CH_4^{\bullet+}$ complex, i.e., $C_2H_8^{\bullet+}$. The qualitative features of the 3-21G potential energy surface remain unchanged when passing to higher computational levels. The calculated stabilization energy of the most stable complex (D_{3d} symmetry, V in Figure 1) decreases by about 20% but still remains rather high, 16.54 kcal/mol (see Table V). The calculated heat of reaction for the overall reaction (eq

---

(17) GAUSSIAN 86: Frisch, M. J.; Binkley, J. S.; Schlegel, H. B.; Raghavachari, K.; Melius, C. F.; Martin, R. L.; Stewart, J. J. P.; Bobrowicz, F. W.; Rohlfing, C. M.; Kahn, L. R.; Defrees, D. J.; Seeger, R.; Whiteside, R. A.; Fox, D. J.; Fleuder, E. M.; Pople, J. A. Carnegie-Mellon Quantum Chemistry Publishing Unit, Pittsburgh, PA, 1984.

(18) Amos, R. D.; Rice, J. E. CADPAC, Issue 4.0, University of Cambridge.

(19) Kimura, K.; Katsumata, S.; Achiba, Y.; Yamazaki, T.; Iwata, S. *Handbook of HeI Photoelectron Spectra of Fundamental Organic Molecules*; Japan Science Society Press: Tokyo; Halsted Press: New York, 1981.

(20) Bahr, J. L.; Blake, A. J.; Carver, J. H.; Kumar, V. *J. Quant. Spectrosc. Radiat. Transfer* **1969**, *9*, 1359.

(21) De Alti, G.; Decleva, P.; Sgamellotti, A. *J. Electron Spectrosc. and Rel. Phenom.* **1977**, *12*, 249. Ragle, J. L.; Stenhouse, I. A.; Frost, D. C.; McDowell, C. A. *J. Chem. Phys.* **1970**, *53*, 178.

(22) Lias, S. G.; Liebman, J. F.; Levin, R. D. *J. Phys. Chem. Ref. Data* **1984**, *13*, 695.

(23) Rühl, E.; Bisling, P.; Brutschy, B.; Baumgärtel, H. *J. Electron Spectrosc. Rel. Phenom.* **1986**, *41*, 411.

Table II. Geometries and Energies of Methyl Chloride and Its Derivatives (SCF/6-31G**//SCF/6-31G**)

molecule	geometry and energy[a]	
	parameter	value
CH_3Cl (XIII)	R_{C-Cl}	1.7848
(C_{3v})	R_{C-H}	1.0872
	$\angle_{HCCl}$	108.4
	energy	−499.09790
	ZPE	0.04038
$CH_3Cl^{\bullet+}$ (XIV)	R_{C-Cl}	1.8682
(C_s)[b]	R_{C-H}	1.0830
	$R_{C-H'}$	1.0772
	$\angle_{ClCH}$	102.4
	$\angle_{H'CH'}$	115.9
	α[c]	119.0
	energy	−498.71944
	ZPE	0.03741
CH_3ClH^+ (XV)	R_{C-Cl}	1.9049
(C_s)[b]	R_{Cl-H}	1.2810
	R_{C-H}	1.0770
	$R_{C-H'}$	1.0756
	$\angle_{CClH}$	101.7
	$\angle_{ClCH}$	101.4
	$\angle_{ClCH'}$	104.8
	$\angle_{HCClH}$	180.
	$\angle_{H'CClH}$	61.1
	energy	−499.34699
	ZPE	0.04910
$CH_2Cl^{\bullet}$ (XVI)	R_{CCl}	1.7173
(C_s)[b]	R_{CH}	1.0705
	$\angle_{ClCH}$	116.6
	$\angle_{HCH}$	122.7
	energy	−498.46472
	ZPE	0.02453
H–Cl (XVII)	R_{H-Cl}	1.2655
($C_{\infty v}$)	energy	−460.06621
	ZPE	0.01425
$CH_3Cl\cdots HCl$ (XVIII)	R_{C-Cl1}	1.7899
(C_s)[b]	R_{Cl1-H1}	2.7308
	R_{H1-Cl2}	1.2685
	R_{C-H2}	1.0778
	R_{C-H3}	1.0781
	$\angle_{CCl1H1}$	99.8
	$\angle_{Cl1H1Cl2}$	157.2
	$\angle_{Cl1CH2}$	108.4
	$\angle_{Cl1CH3}$	108.1
	$\angle_{H3CCl1H1}$	120.0
	energy	−959.16712
	ZPE	0.04889

[a] Energies are in au, bond distances in Å, angles in deg, and frequencies in cm^{-1}. [b] See figure for definition of atoms. [c] Angle made by Cl–C and the bisector of the H–C–H plane.

Table III. Ionization Potentials (eV)

process	potential[a]	calcd[b]	exptl[c]
$CH_4 \rightarrow CH_4^{\bullet+} + e$	a	12.580	12.616
	v	14.229	14.57
$CH_3F \rightarrow CH_3F^{\bullet+} + e$	a	12.376	12.5–12.7
	v	13.283	13.31
$CH_3Cl \rightarrow CH_3Cl^{\bullet+} + e$	a	11.179	11.29
	v	11.019	11.29

[a] a and v stand for adiabatic and vertical. [b] MP4/6-31G**//MP2/6-31G** for CH_4 and CH_3F, MP4/6-31G**//SCF/6-31G** for CH_3Cl. [c] References 19–21.

Table IV. Energies of Protonation and Proton Affinities (kcal/mol)

	ΔE	ΔH_0[c]	PA[d]
$CH_4 + H^+ \rightleftarrows CH_5^+$	132.5[a]	128.2	132.0
$CH_3F + H^+ \rightleftarrows CH_3FH^+$	155.2[a]	149.0	150.0, 129 ± 3[f]
$CH_3Cl + H^+ \rightleftarrows CH_3ClH^+$	159.8[b]	154.3	163
$CH_3^{\bullet} + H^+ \rightleftarrows CH_4^{\bullet+}$	132.8[a]	126.9	
$CH_2F^{\bullet} + H^+ \rightleftarrows CH_3F^{\bullet+}$	133.0[a,e]	127.9	
$CH_2Cl^{\bullet} + H^+ \rightleftarrows CH_3Cl^{\bullet+}$	160.2[b,e]	152.1	

[a] MP4/6-31G**//MP2/6-31G**. [b] MP4/6-31G**//SCF/6-31G**. [c] ZPE included. [d] Experimental values[22] at 298 K. [e] Protonization energy for C-protonization. [f] Reference 23.

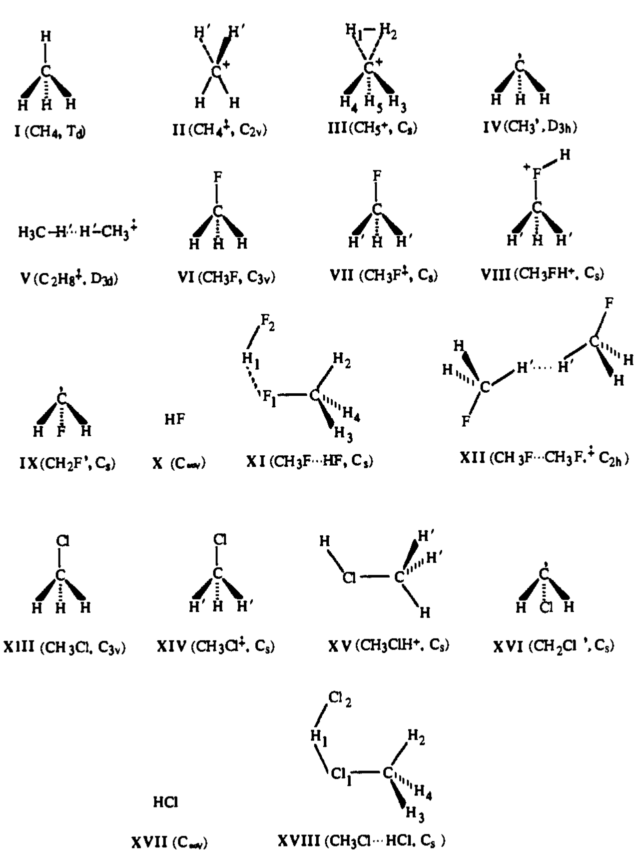

Figure 1. List of the studied species.

Table V. Stabilization Energy (ΔE^S) and Enthalpy (ΔH_0^S) and Reaction Energy (ΔE^R) and Enthalpy (ΔH_0^R) for the Processes[a] (kcal/mol) $CH_3X + CH_3X^{\bullet+} \rightleftarrows C_2H_6X_2^{\bullet+} \rightleftarrows CH_4X^+ + CH_2X^{\bullet}$ (kcal/mol)

X	ΔE^S (ΔH_0^S)	ΔE^R (ΔH_0^R)	ΔH^R(exp)
H	−15.96[b] (−16.54)[c,d]	0.28[b] (−1.78)[f]	−4.16[h] −6[i]
F	−14.2[b] (−12.3)[e]	−22.19[b] (−21.03)[f]	
Cl		0.33[g] (−2.28)[f]	−4.9[j]

[a] Stabilization refers to formation of the $C_2H_6X_2^{\bullet+}$ intermediate; the remaining values refer to the overall reaction. [b] MP4/6-31G**//MP2/6-31G** (frozen core). [c] ΔH_0 at 0 K: ZPE and BSSE included. [d] 3-21G value of ΔE^S equals −21.31 kcal/mol. [e] ZPE and BSSE obtained at SCF/6-31G**//SCF/6-31G**. [f] ΔH_0 at 0 K: ZPE included. [g] MP4/6-31G**//SCF/6-31G**. [h] Reference 7. [i] Reference 11. [j] Reference 5.

1, X = H) was significantly improved; the best calculated value (−1.781 kcal/mol) differs from the two observed values[7,11] by 2.38 and 4.22 kcal/mol, respectively (Table V).

It is tempting to compare the interaction between methane and its radical cation and the association between methane and the CH_5^+ cation. Experimental[24] as well as theoretical[25,26] values for the latter are available. The structure[25,26] of the $CH_4{\cdot}CH_5^+$ complex reminds one of $CH_4{\cdot}CH_4^{\bullet+}$; either H^+ or H_2 separate the two carbon-containing units. However, the 6-31G**//3-21G interaction energy,[26] which amounts to −3.3 kcal/mol, represents only about one-fifth of the interaction energy between CH_4 and $CH_4^{\bullet+}$.

The recently studied reaction of CH_3F with $CH_3F^{\bullet+}$ (eq 1, X = F)[4] is according to our calculations significantly more exothermic (−21 kcal/mol, see Table V) than that of methane with its radical cation (eq 1, X = H). The stabilization of the $C_2H_6F_2^{\bullet+}$ complex amounts to −14.2 kcal/mol. The reaction of CH_3Cl with $CH_3Cl^{\bullet+}$ (eq 1, X = Cl) is predicted to be energetically close to

---

(24) Hiraoka, K.; Mori, T. *Chem. Phys. Lett.* **1989**, *161*, 111 (in this paper previous experimental and theoretical works are cited).

(25) Yamabe, S.; Osamura, Y.; Minato, T. *J. Am. Chem. Soc.* **1980**, *102*, 2268.

(26) Fois, E.; Gamba, A.; Simonetta, M. *Can. J. Chem.* **1985**, *63*, 1468.

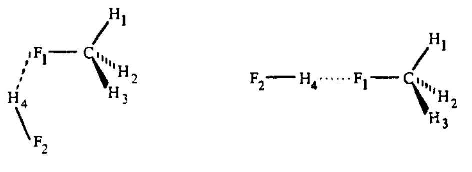

XIa XIb

Figure 2. Activated complex (XIa) represents a barrier to rotation of the methyl group in the hydrogen-bonded complex (XI) and the second-order saddle point (XIb) possesses a linear structure.

that of the parent system (eq 1, X = H). As in the case of the parent system there is quite good agreement between calculated and observed energy changes (Table V).

A minimum for the complex $C_2H_6F_2^{\bullet+}$ was located at the SCF level with the 3-21G and 6-31G** basis sets and at the MP2 level (6-31G**). In all cases a "bent" structure with C_{2h} symmetry (see XII in Table I and Figure 1) was found. Comparison of the structure of XII with that of the parent system (V in Table I and Figure 1) indicates that, with the exception the "bent" nature of XII, the two systems are very similar. Both at the SCF/6-31G** level have a short internal H···H bond (0.9712 Å in V and 0.9722 Å in XII) and a relatively long bond (1.2825 Å in V and 1.3111 Å in XII) between the carbons and the internal hydrogens. It should be noted that XII has one frequency computed to be zero. The normal mode of this vibration corresponds to a rotation of the CH_2F groups, which indicates that there is essentially free rotation of the CH_2F groups in XII. The corresponding frequency in V (methyl rotation) while not zero is very low (21 cm^{-1}).

Two additional structures for the radical cation dimer methyl fluoride were considered. With a C_{2h} symmetry constraint a stationary point for a cyclic form was located with the SCF/3-21G basis set:

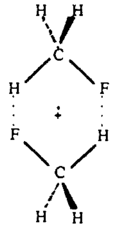

XIX

However, a vibrational analysis showed it to be a saddle point. The other structure was one in which the two "internal" atoms of the complex were hydrogen and fluorine (XX). No minimum (3-21G) could be located for such a structure.

$$CH_3—F\cdots H—CH_2F^{\ddagger}$$

XX

In contrast to CH_4 and CH_3F, our attempts to find a minimum on the potential energy surface for the radical cation dimer of CH_3Cl failed. A plausible explanation for this was found in the literature.[13,27] With alkyl bromides and iodides, association reactions (i.e., formation of radical cation dimers) are not preceded by proton transfer. In CH_3Cl, however, a proton transfer is observed, and no $(CH_3Cl)_2^{\bullet+}$ is formed up to 0.5 Torr.

In the future we would like to compare reaction and stabilization energies in the series of reactions H_2 and $H_2^{\bullet+}$, HF + HF$^{\bullet+}$, and HCl + HCl$^{\bullet+}$ with the interaction between the corresponding methylated species, i.e., $CH_4 + CH_4^{\bullet+}$, $CH_3F + CH_3F^{\bullet+}$, and $CH_3Cl + CH_3Cl^{\bullet+}$.

Because of our interest in anion–molecule reactions an attempt was made to investigate the analogous anion radicals. It turned out, however, that $CH_3F^{\bullet-}$ and $CH_3Cl^{\bullet-}$ dissociated into halide ions and the methyl radical. This finding is supported by a very recent MCSCF ab initio study of the C–Cl bond cleavage in methyl chloride.[28] The anion formed in a reductive dehalogenation dissociates immediately into $CH_3^{\bullet}$ and Cl$^-$.

Table VI. Calculated ΔE and ΔH_0 Values of $CH_3F{\cdot}HF$[a] and $CH_3Cl{\cdot}HCl$[b] Formation from Free Components at 0 K (kcal/mol)

	H.F.	MP2	MP3	MP4
ΔE(F)	−6.58	−9.14	−8.42	−9.08
ΔE(Cl)	−1.89	−2.62	−2.49	−2.55
$\Delta H_0{}^c$(F)	−2.76 (−0.39)	−4.80 (−0.43)	−4.08 (−0.20)	−4.74 (−0.28)
$\Delta H_0{}^c$(Cl)	−0.15 (−0.08)	−0.88 (−0.21)	−0.75 (−0.07)	−0.81 (−0.10)

[a] SCF/6-31G**//SCF/6-31G** and MPn/6-31G**//MP2/6-31G** values. [b] SCF/6-31G**//SCF/6-31G** and MPn/6-31G**//SCF/6-31G** values. [c] ZPE included; values in parentheses also include BSSE correction.

Table VII. Computed Vibrational Frequencies and IR Intensities[a]

CH_3–H···H–$CH_3^{\bullet+}$ (V)[b]			FCH_2–H···H–$CH_2F^{\bullet+}$ (XII)[b]			CH_3F···HF (XI)[c]		
sym	ν	int	sym	ν	int	sym	ν	int
A_{1u}	21	0	A_u	0		A″	57	0.0
E_u	207	0.4	B_u	74	32.4	A′	151	18.3
E_u	207	0.4	A_g	137	0	A′	234	16.9
A_{1g}	404	0	A_u	233	0.0	A″	513	140.6
E_g	518	0	A_g	471	0	A′	680	233.2
E_g	518	0	B_g	596	0	A′	1062	81.4
E_g	1040	0	B_u	988	587.5	A″	1223	1.3
E_g	1040	0	A_u	1139	1.1	A′	1231	1.5
E_u	1104	10.0	B_u	1182	937.0	A′	1540	2.2
E_u	1104	10.0	B_g	1191	0	A′	1563	2.5
A_{2u}	1148	0	A_g	1204	0	A″	1572	2.7
A_{1g}	1378	0	B_g	1308	0	A′	3164	22.9
E_u	1525	20.8	A_u	1311	18.7	A″	3278	24.3
E_u	1525	20.8	A_g	1349	0	A′	3295	9.6
E_g	1527	0	B_u	1358	236.9	A′	4031	349.6
E_g	1527	0	A_g	1389	0			
A_{2u}	1682	352.2	B_u	1607	53.2			
A_{1g}	2588	0	A_g	1633	0			
A_{2u}	3231	17.1	B_u	1661	180.6			
A_{1g}	3233	0	A_g	2313	0			
E_u	3404	27.2	B_u	3264	48.6			
E_u	3404	27.2	A_g	3269	0			
E_g	3405	0	A_u	3402	11.0			
E_g	3405	0	B_g	3403	0			

[a] Frequencies in cm^{-1}; intensities in km mol^{-1}. [b] SCF/6-31G**//SCF/6-31G**. [c] MP2/6-31G**//MP2/6-31G**.

Complexes with Proton Donors and Their Vibrational Spectra. A complex between methane and proton donors like HF and HCl is, no doubt, a typical van der Waals molecule and will not be investigated in this work. The still unknown complex between CH_3F and HF, however, is of interest to molecular spectroscopists.[16] On the basis of an electrostatic model a linear arrangement of subunits was expected as a consequence of dipole–dipole attraction. It turns out, however, that the linear complex (XIb in Table I and Figure 2) represents only a saddle point of second order (SCF/6-31G**). The real minimum has a nonlinear structure (XI in Table I and Figure 1); another stationary point (XIa in Table I and Figure 2) was located 0.1 kcal/mol (SCF/6-31G**) above the minimum. It is a first-order saddle point and represents a nearly negligible barrier to rotation of the methyl group in the hydrogen-bonded complex. ΔE and ΔH_0 values accompanying formation of the $CH_3F{\cdot}HF$ complex are summarized in Table VI.

The $CH_3Cl{\cdot}HCl$ (XVIII in Table II and Figure 2) complex is a very weak van der Waals molecule characterized by a reaction heat accompanying its formation from free molecular components, CH_3Cl and HCl, of about −0.1 kcal/mol (Table VI). The nature of the complex manifests itself in the calculated vibrational frequencies (see supplementary material). It is easily possible to determine which frequencies are due to perturbed subsystems (alkylhalogenides and HF or HCl); the five lowest energy vi-

---

(27) Reference 1, p 189.

(28) Benassi, R.; Bernardi, F.; Bottoni, A.; Robb, M. A.; Taddei, F. *Chem. Phys. Lett.* **1989**, *161*, 79.

brations are due to intermolecular vibrations. These intermolecular vibrations should be sought in the regions of 50–700 cm^{-1} and 20–500 cm^{-1} for $CH_3F{\cdot}HF$ and $CH_3Cl{\cdot}HCl$, respectively.

Finally, there is a real possibility of recording low-temperature vibrational spectra of the radical cation dimers of methane (V) and methyl fluoride (XII) in rigid inert matrices and to study gas-phase vibrational spectra of the $CH_3F{\cdot}HF$(XI) complex.[16] Computed vibrational frequencies and IR intensities are summarized for these species in Table VII. These frequencies have not been scaled, and therefore they are likely to be higher than the experimental values by 5–10%.[29]

---

(29) Hess, B. A., Jr.; Schaad, L. J.; Crsky, P.; Zahradnik, R. *Chem. Rev.* **1986**, *86*, 709.

Acknowledgment. Our thanks are due to Professor S. Suzuki (IMS, Okazaki) for drawing our attention to his recent studies of CH_3Cl^+ and for informing us about the reactivity of CH_3F^+ prior to publication. B.A.H. thanks the National Science Foundation for an instrument grant used to purchase an SCS-40 computer on which the calculations reported here were performed.

Supplementary Material Available: A table of SCF/6-31G** geometries, vibrational frequencies, and energies and MP2/6-31G**//MP2/6-31G** frequencies of I–XI, a table of SCF/6-31G**//SCF/6-31G** frequencies of XII–XVIII, a table of MP2-, MP3-, and MP4/6-31G**//MP2/6-31G** energies of I–XI, and a table of MP2-, MP3-, and MP4/6-31G**//SCF/6-31G** of XII–XVIII (8 pages). Ordering information is given on any current masthead page.

Penning Ionization Electron Spectroscopy of *n*-Alkane Ultrathin Films. Molecular Orbitals and Orientation of Molecules

Hiroyuki Ozaki*,[†] **and Yoshiya Harada**[‡]

Contribution from the Department of Chemistry, College of General Education, Nagoya University, Chikusa, Nagoya 464-01, Japan, and the Department of Chemistry, College of Arts and Sciences, The University of Tokyo, Komaba, Meguro, Tokyo 153, Japan.

Received October 30, 1989

Abstract: Penning ionization electron spectra (PIES) were measured for evaporated ultrathin films [4 (monolayer) to 200 Å thick] of long-chain *n*-alkanes. The electron distributions as well as the energies of three types of MOs (pseudo-π, σ_{2p}, and σ_{2s}), obtained by ab initio MO calculations, could be surveyed experimentally by PIES; the agreement between the calculated and experimental results was fairly good. The valence electronic structure of long-chain *n*-alkanes is characterized by the high density of states of the pseudo-π and σ_{2s} MOs, which were predominantly detected for monolayer films made up of flat-lying molecules. For crystalline films comprised of molecules standing upright, MOs with large distribution on the terminal hydrogen atom were exclusively detected. These data serve for the PIES characterization of various molecular aggregates of alkane derivatives, including Langmuir–Blodgett films. Ultraviolet photoelectron spectra were also measured, but unlike PIES, they were severely influenced by substrate signals and/or conduction band structures. It was demonstrated that Penning spectroscopy probes occupied orbitals selectively.

Introduction

n-Alkanes are among the most fundamental organic compounds, and their fragments, alkyl groups, are contained in many chemical substances. Furthermore, Langmuir–Blodgett (LB) films[1,2] and some polymers mainly consist of alkyl chains. To develop a molecular organism of an alkane derivative with a new function, the electronic structures of the constituent molecule must be elucidated. The electronic structure of long-chain *n*-alkanes has been studied as a model to simulate that of polyethylene.[3–9] Since the *n*-alkane having 13 carbons, tridecane, gave an X-ray photoelectron spectrum similar to that of polyethylene, 10 carbons or so were considered to be sufficient to simulate the infinite chain of polyethylene.[3,4] Therefore, the results of electron spectroscopic measurements for *n*-alkanes have been interpreted on the basis of band calculations for polyethylene.[5–8] We plan here, however, to show that the valence electronic structure of *n*-alkanes viewed with the molecular orbital picture can be explored experimentally by Penning ionization electron spectroscopy.

The kinetic energy analysis of electrons ejected by collisions between target molecules M and metastable rare gas atoms, e.g., He* (2^3S) with excitation energy 19.82 eV, ($M + He^* \rightarrow M^+ + He + e^-$) provides a Penning ionization electron spectrum (PIES).[10] In this ionization process, an electron in an MO of M transfers to the vacant 1s AO of He*, and an electron in the 2s AO of He* is ejected simultaneously to an orbital of the continuum state.[11] The process is illustrated for solid-phase molecules in Figure 1. Since metastables do not permeate into the solid and the transition probability is governed by the spatial overlap of the relevant MO and the helium 1s AO, an MO spreading outside the repulsive (van der Waals) surface of molecules in the outermost layer provides a stronger band in the PIES than an MO distributed inside the surface. Accordingly,

---

[†] Nagoya University.

[‡] The University of Tokyo.

(1) Blodgett, K. B. *J. Am. Chem. Soc.* **1935**, *57*, 1007–1022.

(2) *Thin Solid Films* **1983**, *99*, 1–329.

(3) Pireaux, J. J.; Svensson, S.; Basilier, E.; Malmqvist, P.-Å.; Gelius, U.; Caudano, R.; Siegbahn, K. *Phys. Rev.* **1976**, *A14*, 2133–2145.

(4) Pireaux, J. J.; Caudano, R. *Phys. Rev.* **1977**, *B15*, 2242–2249.

(5) Seki, K.; Hashimoto, S.; Sato, N.; Harada, Y.; Ishii, K.; Inokuchi, H.; Kanbe, J. *J. Chem. Phys.* **1977**, *66*, 3644–3649.

(6) Seki, K.; Ueno, N.; Karlsson, U. O.; Engelhardt, R.; Koch, E. E. *Chem. Phys.* **1986**, *105*, 247–265, and references therein.

(7) Ueno, N.; Fukushima, T.; Sugita, K.; Kiyono, S.; Seki, K.; Inokuchi, H. *J. Phys. Soc. Jpn.* **1980**, *48*, 1254–1260.

(8) Ueno, N.; Sugita, K.; Kiyono, S. *Chem. Phys. Lett.* **1981**, *82*, 296–300.

(9) Hashimoto, S.; Seki, K.; Sato, N.; Inokuchi, H. *J. Chem. Phys.* **1982**, *76*, 163–172.

(10) Čermák, V. *J. Chem. Phys.* **1966**, *44*, 3781–3786.

(11) Hotop, H.; Niehaus, A. *Z. Phys.* **1969**, *228*, 68–88.

0002-7863/90/1512-5735$02.50/0